Assessment and Design of Frequency Containment Reserves with HVDC Interconnections

Danilo Obradović, Mehrdad Ghandhari
Electric Power and Energy Systems Department
KTH Royal Institute of Technology
Stockholm, Sweden
daniloo@kth.se, mehrdad@kth.se

Robert Eriksson
Market and System Development
Swedish National Grid
Sundbyberg, Sweden
robert.eriksson@svk.se

***Abstract*—Frequency control is one of the main actions in power system operation, since large frequency deviation from the nominal value can lead to automatic frequency protection triggering to avoid equipment damaging. The three main factors which affect the dynamical response of the frequency include the amount of power imbalance due to a disturbance, available reserves and total inertia of the system. Due to increased integration of renewable energy sources, the total inertia of the system decreases and makes the speed of the response more sensitive to power balance disturbances. This paper assesses the dynamical performance of generators involved in the Frequency Containment Reserves and correlates them with additional Emergency Power Control from High Voltage Direct Current (HVDC) interconnections. The currently used constant power ramp control and a new proposed frequency droop control of HVDC interconnections are investigated for different amounts of inertia in a test system representing the Nordic Power System. The performance of each HVDC control is evaluated with respect to the maximum Instantaneous Frequency Deviation and the amount of power required for provided frequency control actions.**

***Index Terms*—Emergency Power Control, Frequency Containment Reserves, HVDC interconnections, Nordic power system**

I. Introduction

With the aim to reduce pollution, future power system will progressively integrate more Renewable Energy Sources (RES) to replace conventional thermal and nuclear productions. Since RES (such as wind power and solar power) are decoupled from the grid by power electronics they do not inherently contribute to the power system inertia which has a significant impact on the Instantaneous Frequency Deviation (IFD). The Frequency Containment Reserve (FCR) is one of the balancing actions to keep the frequency within acceptable limits. The objective of the FCR (also known as primary control) is to stabilize the system frequency within a short time interval after a disturbance. Related to that, maximum Steady-State Frequency Deviation (SSFD) and maximum IFD are defined.

In a system with a low inertia, the Rate of Change of Frequency (RoCoF) will be large after a large power balance disturbance (such as loss of a large generator). A large RoCoF will result in a larger IFD which may activate frequency protection systems to apply under frequency load shedding and/or generator tripping. Such disconnections are not desirable in a modern society.

During large disturbances, the mechanical power must contain an appropriate dynamic response which has the capability to meet the power balance before the frequency leaves allowed range. In power systems with low inertia, a time frame for the required power balance is just a few seconds. Taking into account the physical properties of the turbine and the water (steam) flow, the governor control must be properly tuned. One of the possibilities to assess the governor capability to enable the appropriate mechanical power output is open loop testing of a unit. The response should be designed so that, for a specified frequency input signals, the desired power output is obtained. The list of conditions that a unit must fulfill is referred to as the unit dynamic requirements. Furthermore, the requirement related to robust stability margin of the closed loop system is also applied. It presents a robust measure to handle the system and control uncertainty. The typical response and a comparison between a hydro and a steam turbine is presented in [1]. In [2], it is investigated why the currently used unit dynamic requirements are not sufficient to keep the IFD within the defined range. As a solution, new requirements, with additional stability margin are defined. Related to that, the governor settings are investigated and appropriate ones are identified.

Beside generators involved in FCR, additional support might come from other elements which possess the ability to supply power into grid following a power balances disturbance. Due to their fast and flexible operation, additional support can be provided from High Voltage Direct Current (HVDC) interconnections in a form of Emergency Power Control (EPC) when they are available for such support. According to [3] HVDC links must be capable to provide frequency support and maintain in normal operating range. In [4], the applied pilot project of the point to point HVDC interconnection is presented with the droop control method. Implementation of the same droop control method of the point to point HVDC links is presented in the following literature. The verification of frequency improvement is verified for different stated models of the power systems.

Without taking into account governor and turbine dynamic and neglecting the voltage dependency, in [5], the focus was

on investigating the impact of the HVDC capacity and rate limit constraints. Relaying on the real measurement data, it is concluded that a low amount of reserved power is sufficient for effective IFD improvement. Also, a similar model is used for the three area system model in [6]. It is presented that changing parameters of one HVDC link or one AC system, affects the frequency response in all connected areas. As a solution, in order to avoid the negative effects in the neighboring systems, frequency control is coordinated from all connected areas. On the other side, some authors included the governor and turbine dynamic, together with voltage dependency. In [7] control is verified and IFD improvement is represented for different cases. Furthermore, in [8] the impact on performance degradation is represented for high time delay and too large droop gains. Also, there have been investigations on the possible modification to the droop control, as an additional lead-lag filter in [9], or integral control as in [10]. Although, improving IFD with additional lead lag, it is presented that electromechanical stability of the receiving end area is reduced. On the other side, a PI controller is verified as an effective solution, but high bandwidth communication system is required.

In [11], an adaptive controller is investigated for HVDC frequency control. It is based on Model Predictive Controller (MPC) and requires only local measurements. Although, for having several links injecting power into the area, modifications of the control settings are needed. It is assumed that the inertia value is known and the RoCoF measurements are reliable. Significant improvements comparing to the droop control method are presented on a model with voltage dependency, a governor and turbine dynamic applied.

Another method is applied in [12] which is based on triggering frequency activation. The HVDC frequency support is executed as a constant ramp power injection. The model contains a single machine equivalent model of NPS with the governor and turbine dynamic included, but no voltage dependency is considered. It is concluded that IFD improvements do not give satisfying results for a given reserved power on HVDC links and new assessments are needed.

This paper provides a frequency control correlation between generators involved in FCR and EPC on HVDC interconnections. The single machine equivalent is applied and the dynamic of the governor and turbine are included. The goal is to reduce the IFD by joint action of FCR units and minimum EPC support. This paper assesses two different HVDC controls methods: the constant ramp power injection with frequency triggering activation and the droop frequency control. Results are provided by taking into account varying inertia values, largest dimensioning incident, and possibilities from HVDC interconnections.

II. System model

In this paper the single machine equivalent model, shown in Fig. 1, is used to study the impact of FCR on the dynamical response of the system frequency. In the figure, $\Delta P_L = \Delta P_{dist}$ represents an active power disturbance in pu and $G(s)$ is the

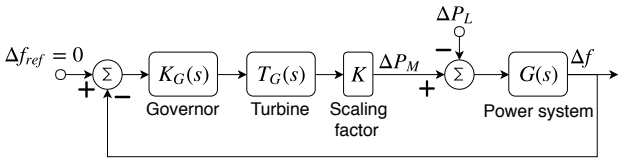

Fig. 1. Single machine equivalent model with FCR

transfer function relating frequency and power which is given by

$$G(s) = \frac{1}{Ms + D} \tag{1}$$

where s is the Laplace operator, Δf is the system frequency deviation in pu and D is the load damping constant. Furthermore,

$$M = 2\,H = 2\,\frac{E_{Ktot}}{S_n} \tag{2}$$

where, H is the system inertia constant given in seconds, E_{Ktot} is the total stored kinetic energy in the system and S_n is the base power.

Also, in Fig. 1 $T_G(s)$ is the transfer function of the linearized model of a hydro turbine which is described by

$$T_G(s) = \frac{1 - T_W Y_0 s}{1 + 0.5 T_W Y_0 s} \tag{3}$$

where, T_W is the water time constant in seconds, Y_0 is the relative loading of the generator and ΔP_M is the turbine mechanical power in pu. Moreover, $K_G(s)$ is the transfer function of a hydro governor which is given by

$$K_G(s) = \frac{(K_P + \frac{K_I}{s} + \frac{K_D \cdot s}{T_f \cdot s + 1})}{(K_P + \frac{K_I}{s} + \frac{K_D \cdot s}{T_f \cdot s + 1})Ep + T_g \cdot s + 1} \tag{4}$$

where, K_P, K_I and K_D are the proportional, integral and derivative parameters of the PID regulator, T_f is the time constant of a high pass filter used for the derivative control part of the PID regulator, T_g is the time constant of the servo motor which controls the gate position, K is a scaling factor and E_P is the droop.

From the figure it can be found that the transfer function relating Δf and ΔP_M is given by

$$R_S(s) = K_G(s) T_G(s) K \tag{5}$$

In steady-state, the following can be obtained

$$\Delta P_M = R_S^{ss}\,\Delta f = \frac{K}{E_P}\,\Delta f \tag{6}$$

Both parameters E_P and K have an impact on the generators regulation strength, also known as frequency bias factor. The purpose of the scaling factor K is to change the amount of reserves continuously. With the minimum scaling factor $K = K_{min}$, reserves are equal to the maximum defined amount of a disturbance ΔP_{dist}.

III. System requirements

A. Frequency requirements

The system frequency requirements are related to IFD Δf_{IFD} and SSFD Δf_{SS} values. These deviations are measured based on the nominal frequency value f_{nom}. The constrains are:

$$|\Delta f_{IFD}| \leq \Delta f_{IFD}^{max};\ |\Delta f_{SS}| \leq \Delta f_{SS}^{max} \tag{7}$$

where, Δf_{IFD}^{max} represents the maximum allowed IFD and Δf_{SS}^{max} the maximum allowed SSFD.

B. Units involved in FCR

In order to achieve a SSFD within the range of Δf_{SS}^{max}, the system must contain appropriate amount of FCR. The FCR is dimensioned according to the largest dimensioning incident with respect to the N-1 criterion, without taking into account the self regulation of loads. Based on this, the minimum regulation strength is given by:

$$R_{S,min} = \frac{\Delta P_{dist}}{\Delta f_{SS}^{max}} \tag{8}$$

R_S can be stated to the higher values and it will provide higher SSFD, but also results in higher FCR costs for operation.

On the other side, two different unit dynamic requirements are represented:

- **Existing requirements (ExR)**:
  - $\Delta P_M(t = 5s) \geq 0.5 \cdot \Delta P_{dist}$
  - $\Delta P_M(t = 30s) \geq \Delta P_{dist}$
- **Designed requirements (DesR)**:
  - $\Delta P_M(t = 5s) \geq 0.93 \cdot \Delta P_{dist}$
  - $\Delta W_M(t = 5s) \geq 1.8s \cdot \Delta P_{dist}$
  - $S_M \leq 2.31$ (for the inertia value $H = 5.22$s)

where, ΔP_M is the mechanical output power, ΔW_M is the mechanical energy output (related to ΔP_M) and S_M is the stability margin, which is defined in [13]. The process of the stated method is represented in the following section and a detailed description is provided in [2].

C. Method for testing units dynamic performances

The aim of this method is to identify which control setting of the equivalent governor will satisfy the frequency deviation and unit dynamic requirements. Only governor control settings E_P, K_P, K_I and scaling factor K are varied. Other parameters are considered constant and are selected based on proposed values in [2].

First, the total droop gain $R_S = R_{S,min}$ is calculated from (8). Further, E_P is selected. Then, the scaling factor $K = K_{min}$ is calculated by:

$$K_{min} = R_{s,min} \cdot E_P \tag{9}$$

The next step is to select K_P and K_I and assess the dynamic response in open loop. If the unit does not fulfill the unit dynamic requirements, it is scaled according to:

$$K_{new} = K_{min} \cdot SC \tag{10}$$

where SC is the scaling capacity factor and K_{new} is a new scaling factor. Having SC larger than one represents a control settings that does not fulfill the mechanical power or energy response requirements. Multiplying the output by SC increases the power output so it reaches the required values. The scaling capacity factor SC must be lower than a value that makes it qualify for robust closed loop stability. After assessing the mechanical power output, with or without increased scaling factor K, the system is checked for stability margin. If a unit satisfies all requirements it is qualified to be involved in the FCR.

D. The Nordic power system

The stated method is investigated on an equivalent representing the Nordic Power System (NPS). The nominal frequency is $f_n = 50$ Hz and the existing and future HVDC interconnections are stated in [14]. The total kinetic energy is in the range of 100 GWs to 300 GWs, given in [15].

In the NPS, FCR is divided into two parts: Frequency Containment Reserves for Normal Operations (FCR-N) and Frequency Containment Reserves for Disturbances (FCR-D). FCR-N deals with the mismatch of the active power in normal operation and operates in the frequency range of 49.9 Hz to 50.1 Hz. FCR-D aims to keep the frequency within the range of 49.0 Hz to 51.0 Hz. The largest disturbance in the NPS is a loss of the largest power plant in the system, with the rated power of $\Delta P_{dist} = 1450$ MW.

FCR-N is considered fully activated, therefore the event starts at a frequency of $f_{(t=0)} = 49.9$ Hz. Related to that frequency, the maximum IFD is $\Delta f_{IFD}^{max} = 0.9$ Hz and the maximum SSFD is $\Delta f_{SS}^{max} = 0.4$ Hz. Using (8), implies that $R_{S,min} = 3625$ MW/Hz. The base power is equal to $S_n = 23$ GW.

E. Results on testing units dynamic requirements in NPS

Using previously defined procedure for evaluating units to qualify for the FCR, or in FCR-D in case of NPS, the results are provided for ExR and DesR in the Fig. (2). The peak of

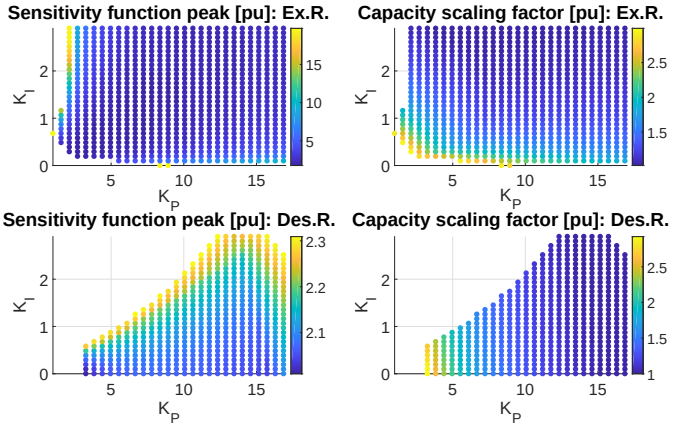

Fig. 2. $[K_P, K_I]$ which satisfy ExR and DesR, for $E_P = 0.06$

the sensitivity function S_M and the capacity scaling factor

SC are illustrated based on the color bar axis. Results are provided for $E_P = 0.06$ pu. Each colored dot represent one set of parameters which satisfies the previously presented requirements. Higher values of SC are presented for units with lower values of K_P and K_I.

In Figs. (3) (ExR) and (4) (DesR), qualified set of K_P and K_I is provided for different values of E_P. The values of frequency minimum are presented for a reduced value of the kinetic energy, equal to 100 GWs ($H = 4.35s$). The

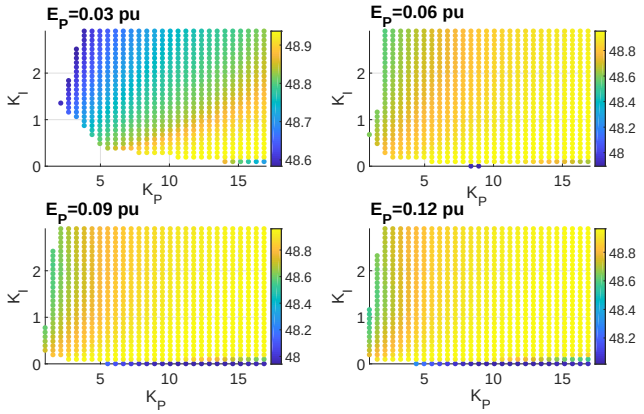

Fig. 3. f_{min} [Hz] for different E_P values and $E_{Ktot} = 100$ GWs - ExR

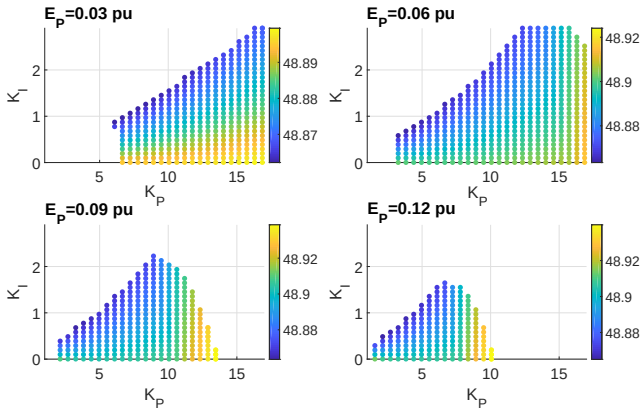

Fig. 4. f_{min} [Hz] for different E_P values and $E_{Ktot} = 100$ GWs - DesR

main purpose of this result is to identify which set of qualified governor parameters gives high IFD value and low capacity scaling value for further analysis and assessment of the HVDC control. Two sets of parameters are chosen:

- **ExR set**: $[E_P; K_P; K_I]_1 = [0.06; 4.9667; 2.61]$ which implies $K_1 = 0.4912$ or $SC_1 = 1.0388$
- **DesR set**: $[E_P; K_P; K_I]_2 = [0.06; 11,2; 2.4617]$ which implies $K_2 = 0.5268$ or $SC_2 = 1.1141$

IV. Constant power ramp control of HVDC

This type of control method is based on frequency triggering activation. When the frequency reaches the triggering level and after a certain time threshold, HVDC interconnections inject additional power into grid with a constant power ramp. This ramp is pre-determined and is not a function of the frequency deviation onces it has been activated. Data settings related to this control, which is currently implemented EPC in NPS, is provided in [12]. The EPC implemented in the HVDC interconnections are distributed in steps. Each step contains a specific power capacity, triggering frequency level, ramp and time threshold. HVDC interconnections involved in EPC are presented in Fig. (5). The control block of one step is

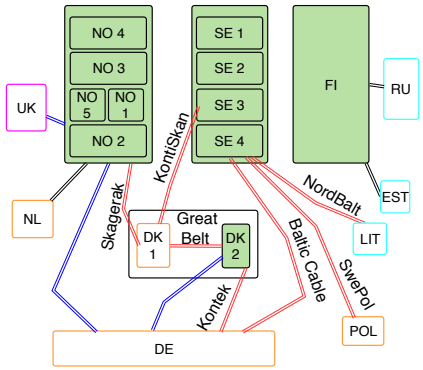

Fig. 5. Green area: NPS; HVDC interconnections: red - involved in EPC, black - not involved in EPC, blue - future interconnections

provided in the figure (6). HVDC dynamic is included with

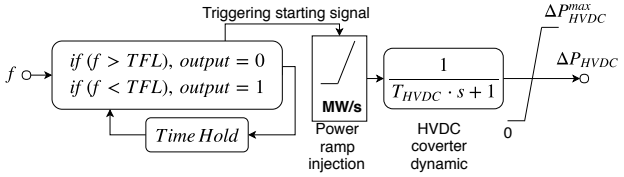

Fig. 6. Block diagram of the constant power ramp control of the HVDC

the time constant $T_{HVDC} = 100$ ms which represent mainly the dynamic of the converters. Power will be increased until the capacity of the step is reached. Although, capacities can vary with respect to the loading of the HVDC cable, in this work it is assumed that the full capacities are available.

A. Contribution of the each link to IFD improvement

One way to test how much one link can contribute to the IFD improvement is to test each link contribution separately for different inertia values. In Table (I) IFD improvements are provided for each link compared to the base case of IFD without EPC support, results provided in Table (III). Results

TABLE I
ONLY ONE LINK ACTIVATED IN EPC (EXR SET)

Link	KS	BC	SP	GB	SK12	SK34	K	NB
[GWs]	IFD improvement [Hz]							
80	0,22	0,13	0,11	0,01	0,06	0,04	0,01	0,23
100	0,20	0,12	0,10	0,01	0,05	0,03	0,01	0,19
125	0,19	0,11	0,08	0,01	0,03	0,02	0,01	0,14
150	0,18	0,10	0,07	0,01	0,02	0,01	0,01	0,10
175	0,17	0,09	0,06	0,01	0,02	0,01	0,01	0,07

marked with green color are ones where $f_{min} > 49$ Hz, and in yellow if $f_{min} < 49$ Hz. The power is injected until the

reserve capacity on the activated link is reached. It means that the power is injected even if the RoCoF is higher than zero. This amount of power is considered as unused, since it does not contribute to an IFD improvement. The percentage of unused power to the maximum injected power is represented in Table (II).

TABLE II
"UNUSED" POWER - RAMP INJECTION AFTER THE f_{min} (EXR SET)

Link	KS	BC	SP	GB	SK12	SK34	K	NB
[GWs]	$EPC_{max,i} - EPC_{f_{min},i}$ [% of $EPC_{max,i}$]							
80	24	33	38	0	42	55	50	0
100	20	32	38	0	42	55	43	0
125	17	32	40	0	46	59	35	0
150	15	34	45	0	56	67	28	4
175	13	37	54	0	54	75	22	40

B. All available links are activated in EPC

All links are activated in the EPC with their full capacity. These results are represented in Table (III). The column

TABLE III
ALL LINKS ARE ACTIVATED IN EPC (EXR SET)

	No EPC	All links in EPC	Total	Unused
[GWs]	$f_{min,no}$ [Hz]	f_{min} [Hz]	[MW]	[%]
80	48,50	48,93	2378	59
100	48,68	49,05	2138	61
125	48,83	49,16	1538	48
150	48,93	49,23	1238	36
175	49,00	49,27	1238	37

named "Total" indicates how much power is injected from all HVDC interconnections, and "Unused" is the percentage of the power injected after the frequency minimum, related to "Total" power.

C. Equivalent ramp control

The currently used control of EPC and generator units are able to provide appropriate IFD values for 100 GWs ($H = 4.35$ s), with assumption that there is enough reserved power on the HVDC interconnections. In can be noted, that for some cases, large amount of power is injected, and a high percentage is not useful for the IFD improvement. This feature is a consequence of low triggering levels and low ramp injections. Their poor performance is clearly notable during activation of only one interconnection.

In the next step, it is assumed that all HVDC interconnections have only one step, the same triggering level and the same time threshold. An additional signal provides information when the frequency minimum is reached and the EPC should therefore not increase the power further. An analysis of the IFD is provided for two cases of governor control settings, which are based on: ExR set in Fig. (7) and DesR set in Fig. (8). These results provide how much reserved power and total ramp rates are needed for enabling the system frequency stability. Higher values of triggering levels imply lower amounts of reserved power, but trigger the EPC more often. It is important that there is information of the frequency minimum, since this information limits further increase of the EPC during the frequency deviation reduction.

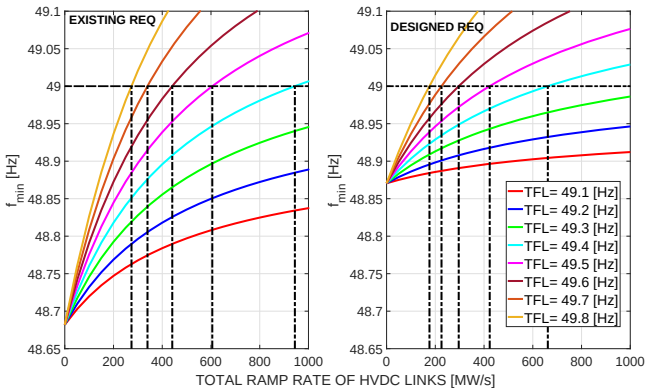

Fig. 7. Equivalent ramp control and f_{min} improvement

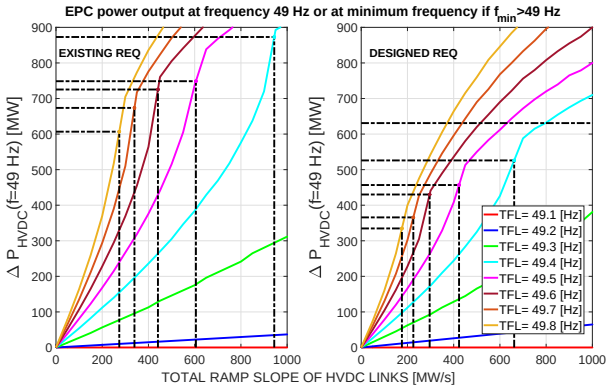

Fig. 8. Equivalent ramp control and needed EPC

V. DROOP FREQUENCY CONTROL OF HVDC LINK

EPC is proportional to the frequency deviation and only local measurements are needed. Block diagram of the used control is in Fig. (9). There is no time threshold and the

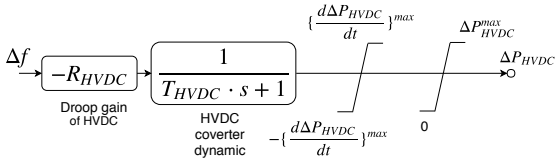

Fig. 9. Block diagram of droop control for HVDC

frequency bandwidth is the same as for the FCR-D. Although, larger droop gain values improve IFD, it may also lead to instability problems, like it is pointed out in [8]. Usually, droop gain is selected to be proportional to HVDC capacity [6]. In this work, however, the aim is to identify the minimum droop gain that will enable frequency stability.

A. Implementing the droop with the same system constrains

It assumed that HVDC links have the same capacity and ramp limits constraints as they have in currently used control. Having low ramp or capacity constraints will affect the performance of EPC. In the case of the Skagerak 3+4 link, in Fig. (10), it is presented that after certain value of droop (around

200 MW/Hz) it will not provide further IFD improvement. Also, in the right figure, it can be seen that total EPC Skagerak

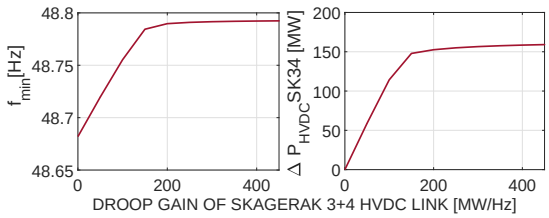

Fig. 10. SK34 activated with droop control and ramp limits affect

3+4 capacity of 260 MW will never be reached regardless the droop gain value. The same behavior and conclusion is stated for all other HVDC links.

B. The equivalent droop method

Avoiding having large droop gain on the certain HVDC link could solve ramp or capacity constrain problem. If there are no constrains then control of all HVDC links can be referred as equivalent droop control. Analysis which provide how much total droop is needed, from as system point of view, is investigated. Different inertia values are tested with ExR set and DesR set cases. Frequency nadir dependency and needed power are provided in Fig. (11) and (12). Obviously,

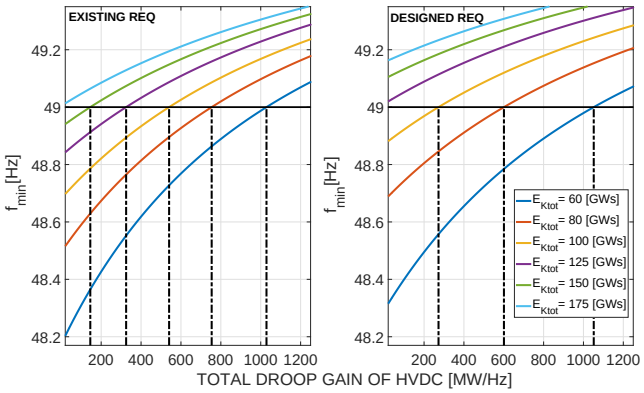

Fig. 11. f_{min} values for equivalent droop control of HVDC

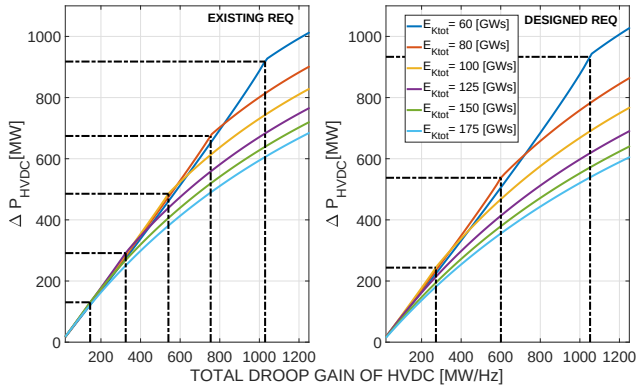

Fig. 12. Power injection for equivalent droop control of HVDC

the lower EPC is needed for droop control of the HVDC and DesR comparing to ramp control and ExR, respectively.

VI. Conclusions

This work analyses the possibilities of two different control methods for HVDC interconnections to improve the frequency stability. It provides which control settings and how much reserved power on the HVDC interconnects are needed for different inertia values. Needed values are related to minimum EPC performance with the aim to keep the IFD within the allowed range for the dimensioning incident. The droop control method demonstrates better performance compared to triggering activation method with constant power injection. The importance of having an appropriate dynamic response of the mechanical power and compliance testing method is presented. A comparison between stating currently used or a new designed method is evaluated. Better performance is obtained with the design method which also takes into account a robust stability margin for the close loop system.

VII. Acknowledgment

This work is supported by the multiDC project, funded by Innovation Fund Denmark, Grant Agreement No. 6154-00020B.

References

[1] P. Kundur, *Power System Stability and Control*, New York: McGraw Hill, 1994, pp. 581-601

[2] M. Kuivaniemi, N. Modig, R. Eriksson, "FCR-D Design of Requirements", ENTSO-E Report, July, 2017.

[3] "NC HVDC - Preliminary Scope: Network on HVDC Connections and DC Connected Power Park Modules", ENTSOE Report, May, 2013.

[4] S. P. Teeuwsen, R. Rössel, "Dynamic Performance of the 1000 MW BritNed HVDC Interconnector Project", IEEE PES General Meeting, pp. 1-8, July, 2010

[5] J. Huang, R. Preece, "HVDC-based Fast Frequency Support for Low Inertia Power Systems", 13th IET International Conference on AC and DC Power Transmission, pp. 1-6, February, 2017

[6] J. E. S. de Haan et al., "Stabilising system frequency using HVDC between the Continental European, Nordic, and Great Britain systems", *Sustainable Energy, Grids and Networks*, vol.5, pp. 125-134, 2016

[7] C. E. Spallarossa, Y. Pipelzadeh, T. C. Green, "Influence of Frequency-Droop Supplementary Control on Disturbance Propagation through VSC HVDC Links", IEEE Power Energy Society General Meeting, pp. 1-5, July, 2013

[8] L. Shen, M. Barnes, R. Preece, J. Milanović, "Frequency Stabilisation using VSC-HVDC", IEEE Power and Energy Society General Meeting, pp. 1-5, July, 2016

[9] A. G. Endegnanew, K. Uhlen, "Global Analysis of Frequency Stability and Inertia in AC Systems Interconnected through an HVDC", 2016 IEEE International Energy Conference, pp. 1-6, April, 2016

[10] O.A. Giddani et al., "Multi-task Control for VSC HVDC power and frequency control", *International Journal of Electrical Power & Energy Systems*, vol. 53, pp. 684 - 690, 2013

[11] L. Papangelis et al., "Decentralized Model Predictive Control of Voltage Source Converters for AC Frequency containment", *International Journal of Electrical Power and Energy Systems*, vol. 98, pp. 342-349, 2018

[12] E. Ørum et al., "Future System Inertia 2", ENTSO-E Report, August, 2016, pp. 31-41, 94-98

[13] S. Skogerstad, I. Postlethwaite, *Multivarible Feedback Control: Analysis and Design*, John Wiley, 2005, pp. 31-35

[14] T. K. Vrana, E. S. Aas, T. I. Reigstad, O. Mo, "Impact of present and Future HVDC Links on the Nordic Power Grid", 13th IET International Conference on AC and DC Power Transmission, pp. 1-6, February, 2017

[15] "Challenges and opportunities for the Nordic power system", Statnett, Fingrid, Energinet.dk, Svenska Kraftnät, Technical Report, August, 2016.